Bioelectrochemistry 79 (2010) 37–42

Contents lists available at ScienceDirect

Bioelectrochemistry

journal homepage: www.elsevier.com/locate/bioelechem

Development of electrochemical DNA biosensor based on gold nanoparticle modified electrode by electroless deposition

Shufeng Liu [a,*], Jing Liu [a], Li Wang [a], Feng Zhao [b]

[a] Key Laboratory of Eco-Chemical Engineering, Ministry of Education, College of Chemistry and Molecular Engineering, Qingdao University of Science and Technology, Qingdao 266042, China
[b] Jiangxi Key Laboratory of Organic Chemistry, Jiangxi Science and Technology Normal University, Nanchang 330013, China

ARTICLE INFO

Article history:
Received 13 April 2009
Received in revised form 14 October 2009
Accepted 21 October 2009
Available online 29 October 2009

Keywords:
Electroless deposition
Gold nanoparticles
DNA hybridization
Electrochemistry

ABSTRACT

In this article, a simple strategy of electroless deposition for gold nanoparticle (Au NP) modification on the conductive substrate is developed. The morphology of Au NP modified electrode could be controlled to some extent by choosing different solution concentrations, deposition times, etc. The Au NP modification increased the electrode surface area largely, and the surface area after Au NP modification on the polyelectrolyte multilayer (PEM) assembled electrode was about 3.3 times that of the planar gold electrode. The enhancement of DNA immobilization and hybridization on the Au NP modified electrode were characterized by cyclic voltammetry (CV) and differential pulse voltammetry (DPV) with the use of $Ru(NH_3)_6^{3+}$ as an electrochemical redox indicator. With this approach, the sensitivity of Au NP modified PEM electrode for target DNA could reach 1×10^{-11} M. Compared with that of planar gold electrode, the detection limit was increased to be about 3 orders of magnitude.

© 2009 Elsevier B.V. All rights reserved.

1. Introduction

Since the concept of DNA biosensor was first introduced [1], the development of DNA biosensors has attracted substantial attentions in connection with research efforts directed at gene analysis, the detection of genetic disorders, tissue matching, forensic applications, etc. [2–9]. Electrochemical technique could offer great advantages over the other existing devices because of its simplicity, rapidness, low-cost and high sensitivity [10–21].

In DNA biosensor fabrication, the immobilization amount of probe DNA on the biosensor interface and further its recognition capability toward complementary DNA play a virtually important role in the DNA biosensor performance [22–26]. In order to upgrade the immobilization amount of probe DNA and improve its DNA hybridization efficiency, different kinds of nanomaterials have been applied for electrode surface modification due to their increased surface area and also beneficial orientation effect for DNA immobilization and recognition [27–30]. Among all the nanomaterials, gold nanoparticles (Au NPs) are the most frequently used for electrode surface modification in the fabrication of biosensor [31,32]. Different strategies have been developed to construct Au NP modified electrode including direct electrochemical deposition, electroless deposition, and assembly by bifunctional chemical linkers, or sol–gel, polymer, etc. For example, Cai et al. [33] assembled the Au NPs (16 nm in diameter) on a cysteamine-modified gold electrode and discovered that the immobilization quantities of thiolated probe DNA on the modified electrode were increased largely than that on a bare gold electrode. Jiang et al.'s group [34,35] also utilized Au NP modified electrode to enhance DNA immobilization and hybridization ability.

In the present paper, we advised a simple electroless deposition method to achieve Au NP modification on the electrode surface. Electroless deposition is a term to describe the spontaneous reduction of metal ions to metallic particles and film in the absence of an external source of electric current [36–38]. The galvanic displacement of electroless deposition occurs by a displacement reaction between solutions of metal salts and immersed metals. The current Au NP modification on the electrode surface could be achieved by using a two-electrode system. One was the Au electrode to be deposited, and another was a sacrificing electrode, currently, copper wire electrode. The Au NPs would be uniformly deposited on the electrode surface with these two electrodes connected by a conductive wire and immersed into the $HAuCl_4$ solution. Apparently, this method for Au NP modification is a simple operation, cost effective, has high throughput, and lacks elaborate equipment compared with other methods. Also, the current method could be used as a general strategy for various metal nanoparticle (Au, Pt, etc.) modifications on different electrode surfaces. The DNA immobilization and hybridization on Au NP modified electrode was detailedly studied with the use of an electro-active complex, $[Ru(NH_3)_6]^{3+}$ (RuHex), which could bind to anionic phosphate of DNA strands through an electrostatic interaction in a stoichiometric approach [39,40]. The developed Au NP modified electrode was convinced to hold a huge potential for further applications in DNA biosensor, immunosensor, etc.

* Corresponding author. Tel./fax: +86 532 84022681.
E-mail address: sliu@qust.edu.cn (S. Liu).

1567-5394/$ – see front matter © 2009 Elsevier B.V. All rights reserved.
doi:10.1016/j.bioelechem.2009.10.005

2. Experimental

2.1. Reagents

The oligonucleotides were purchased from Shanghai Sangon Biological Engineering Technology and Services Ltd. (China); their base sequences are as follows:

Probe DNA: HS-$(CH_2)_6$-5′-TTT TTT GGT GAG GAGG-3′;
Target DNA: 5′-CCT CCT CAC CAA AAA A-3′; and
Non-complementary target DNA: 5′-ATG AAC CTG AGG CCCA-3′.

Mercaptohexanol (MCH), hexaammineruthenium (III) chloride ($[Ru(NH_3)_6]^{3+}$, RuHex), mercaptopropionic acid (MPA), poly(allylamine hydrochloride) (Mw~50,000) (PAH), and poly(styrene sulfonate) (Mw~70,000) (PSS), were purchased from Sigma (USA). All other chemicals such as KNO_3, $K_3Fe(CN)_6$, NaCl, Cu wire (99.99% purity), $HAuCl_4 \cdot 3H_2O$, etc., were of analytical reagent grade and obtained from Beijing Chemical Reagent Company (China). Solutions were prepared with doubly distilled water.

2.2. Apparatus

Electrochemical experiments were performed with a CHI 832b electrochemical analyzer (Shanghai CH Instrument Company, China) using a three-electrode system consisting of a planar gold electrode with an apparent surface area of 20 mm^2 or Au NP modified electrode, a Pt wire as counter electrode, and an Ag/AgCl reference electrode. All experiments were carried out under an inert atmosphere by bubbling nitrogen gas through the working compartment. The solution pH was measured with a model PHS-25 digital acidimeter (Shanghai Leici Factory, China). Scanning electron microscopy (SEM) (Hitachi S-4300) was used to examine the morphology of Au NP modified electrodes.

2.3. Electroless deposition of Au NPs on the planar gold and polyelectrolyte multilayer (PEM) modified electrode surface

Prior to Au NP modification, the Au electrode was firstly polished sequentially with 1, 0.3, and 0.05 μm α-Al_2O_3 paste, and rigorously rinsed with doubly distilled water following each polish. The polished electrode was then cleaned ultrasonically sequentially in water and 95% ethanol for 3 min. Then the polished electrode was connected with a sacrificing electrode (Cu wire) by a conductive wire. Both electrodes were immersed into the 1 mM $HAuCl_4$ solution for the achievement of Au NP electroless deposition on the polished electrode. KNO_3 was added into the above $HAuCl_4$ solution as an electrolyte additive. After a given time, the deposited electrode was taken out and rinsed completely with doubly distilled water.

The process of polyelectrolyte multilayer (PEM) formation on electrode was as follows: the pretreated gold electrode was firstly assembled with a monolayer of mercaptopropionic acid (MPA) by immersing into a 1 mM MPA aqueous solution for 1 h. Then the electrode was alternately dipped in aqueous solutions of PAH (1 mg/mL) and PSS (1 mg/mL) for 15 min, with intermediate water rinsing and N_2 drying. The dipping was repeated until the desired number of bilayers (each bilayer repeat unit consists of one PSS layer and one PAH layer) was achieved. The outermost layer was always PAH layer. The electroless deposition of Au NPs onto PEM assembled electrode was the same procedure with that on the planar gold electrode.

2.4. DNA immobilization and hybridization

The immobilization of probe DNA on the planar or Au NP modified electrodes was performed by incubation of electrodes into a phosphate-buffered saline (PBS) solution (pH 6.83, 50 mM NaCl) containing 0.01 mM of probe DNA for 5 h. Then, the modified electrodes were rinsed successively with PBS solution and distilled water, and dried with nitrogen gas. The probe DNA-modified electrodes were further treated with 1 mM MCH aqueous solution for 2 h to obtain a well aligned DNA monolayer. The probe DNA and MCH modified electrodes were then immersed into the PBS solution containing the target DNA for 1 h at room temperature to form double-stranded DNA (dsDNA) modified electrodes. After that, dsDNA-modified electrodes were washed successively with PBS solution and distilled water, and then dried with nitrogen gas.

2.5. Electrochemical measurement using $[Ru(NH_3)_6]^{3+}$ as the electrochemical indicator

The cyclic voltammograms of the probe DNA or dsDNA-modified electrodes were recorded in 50 μM RuHex of Tris–HCl aqueous solution (0.2 M, pH = 7.4) containing 0.1 M KCl as electrolyte. The DPV experiments were executed in 3.5 μM RuHex of Tris–HCl aqueous solution with the following parameters: the initial potential was 0.20 V; the high potential was 0.2 V; the low potential was −0.5 V; the pulse amplitude was 0.05 V; the pulse period was 0.2 s; and the quiet time was 2 s.

3. Results and discussion

3.1. Electroless deposition of Au NPs on the conductive substrate

Au NP modified electrode could be easily achieved by employing current strategy of electroless deposition. The nucleation and growth of Au NPs deposited on the platinum plate have been studied by quartz crystal microbalance (QCM) method [37]. The size and morphology of deposited Au NPs could be controlled to some extent by choosing different solution concentrations, deposition times and stirring or not. The gradual dissolution of copper from copper sacrificing electrode should be an impetus for the deposition of Au NPs on the electrode surface. Thus, the galvanic displacement reaction should firstly occur onto the surface of sacrificing electrode and then the goal electrode connected to the copper sacrificing electrode. Followed with the process of electroless deposition, the copper surface would be partially displaced by gold and then lose its activity in $HAuCl_4$ solution. Due to the large surface area of employed copper sacrificing electrode, it was sufficient for the success of electroless deposition of Au NPs on the goal electrode surface. The electroless deposition method has been largely used to deposit noble metal nanoparticles on different conductive or non-conductive substrates. The electroless deposition occurring on the conductive substrate usually involves the first deposition of more reductive metal adlayer and then galvanic displacement with acid solution of noble metal salt; or is executed by directly immersing the more reductive metal substrate into the acid solution of noble metal salt. Compared with the reported complicated electroless deposition method, the current strategy for Au NP modification was easier to operate and could be used as a general strategy for Au NP modification on different conductive substrates. It has been previously demonstrated that the deposition amount of Au NPs was in direct proportion to the deposition time by the QCM method.

Fig. 1 shows the typical SEM images of Au NPs deposited on the planar gold electrode (a and b) and PEM electrode (c and d). Both electrodes were obtained by electroless deposition in 1 mM $HAuCl_4$ for 6 min. The planar gold electrode surface was comparably smooth and no gold nanoparticles could be seen (image not shown). Following electroless deposition on the planar gold electrode in 1 mM $HAuCl_4$ for 6 min, the Au electrode was observed to be occupied uniformly by Au NPs with a diameter of about 30–50 nm. The feasibility of current strategy for Au NP modification was also evidenced on the PEM assembled electrode. The gold electrode was layer-by-layer assembled with three bilayers of PSS and PAH and then underwent electroless deposition of Au NPs. It was interestingly found that the novel Au NPs

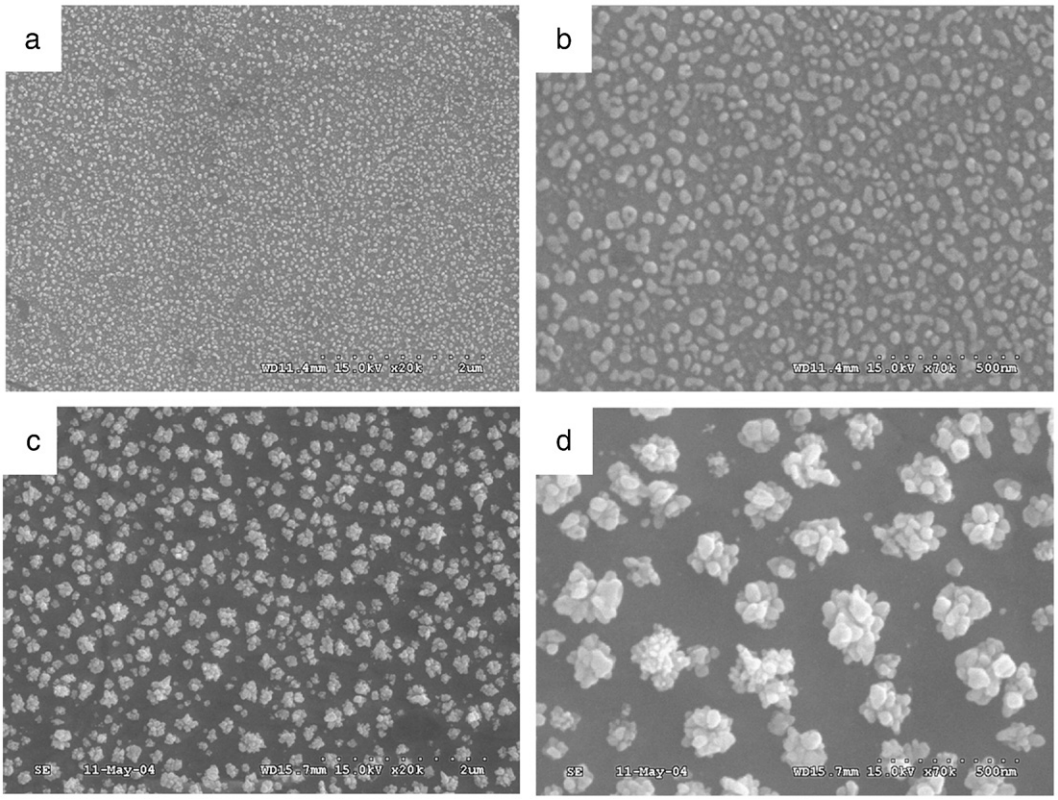

Fig. 1. SEM images of Au NPs obtained by electroless deposition onto planar gold electrode (a, b) and PEM (three bilayers of PSS and PAH) modified electrode (c, d) for 6 min in 1 mM $HAuCl_4$. (b) and (d) are the corresponding high magnification images of (a) and (c), respectively.

distributed with a size of about 100–200 nm were obtained onto the PEM electrode. From high magnification SEM image (see Fig. S1 in Appendix A), it was further observed that the Au NPs actually consisted of many small gold nanoparticles. The PEM bilayer number had an important impact on the morphology of deposited Au NPs (See Fig. S2 in Appendix A). Zhang et al. [41,42] have obtained the novel gold and silver nanostructures onto the PEM matrix modified electrode by electrodeposition. Qian et al. [43,44] also achieved the novel Pt and Pt–Au bimetallic nanostructures onto the polyamidoamine dendrimers matrix modified electrode by electrodeposition. The PEM has been proved to be able to affect the morphology of deposited metal nanoparticles. During current electroless deposition process, the growth of Au NPs was considered to take a progressive nucleation process onto the PEM modified electrode. The PEM could be in favor of the adsorption of anions and play a significant role in the nucleation and growth rate of Au NPs. During the process, seed nucleation was slow and new nuclei continuously formed, which resulted in the formation of nanostructures consisting of many small nanoparticles. This gold nanostructure was not observed by direct electroless deposition onto the planar gold electrode. In particular, the PEM could improve the adhesion stability of deposited Au NPs on the electrode surface. But, the detailed mechanism was not clear and needed further study.

Fig. 2 shows the CV responses of the planar gold electrode, Au NP modified planar electrode, and Au NP modified PEM electrode in N_2-saturated 1 M H_2SO_4 solution. The relative surface area could be evaluated from the coulombic integration of the reductive waves of gold oxide [45]. It could be deduced from Fig. 2 that the ratio of relative surface area of the Au NP modified PEM electrode:Au NP modified planar electrode:planar gold electrode is about 3.3:2.3:1.

3.2. DNA immobilization and hybridization on Au NP modified electrode

The electron transfer of ferricyanide through the modified electrode could be used as a valuable tool to provide some important information about probe DNA immobilization. Fig. 3 shows the cyclic voltammograms obtained for probe DNA modified electrodes in 1 mM $[Fe(CN)_6^{3-/4-}]$ aqueous solution containing 0.1 M KCl at the scan rate of 100 mV s^{-1}. The bare Au electrode witnessed a pair of well-defined redox peaks with the anodic (E_{pa}) and cathodic (E_{pc}) peak potential of 0.28 V and 0.13 V, respectively, and a peak potential difference of 150 mV (curve a). These peaks could be definitely attributed to the redox behaviors of $[Fe(CN)_6^{3-/4-}]$. The electron transfer ability of $[Fe(CN)_6^{3-/4-}]$ could be improved by Au NP modification, which was evidenced by an increase of the voltammetric responses of $[Fe(CN)_6^{3-/4-}]$ on Au NP modified electrode than that of bare electrode (curve b). The

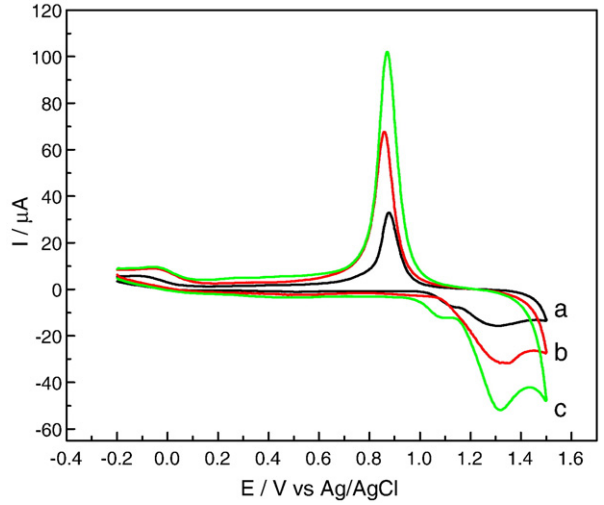

Fig. 2. Cyclic voltammogram for three different electrodes in aqueous 1 M H_2SO_4 solution. (a) Planar gold electrode; (b) Au NP modified planar electrode; (c) Au NP modified PEM electrode (3 bilayers of PSS and PAH). The electroless deposition of Au NPs on planar and PEM electrodes were both conducted for 6 min in 1 mM $HAuCl_4$. Scan rates were all 100 mV/s.

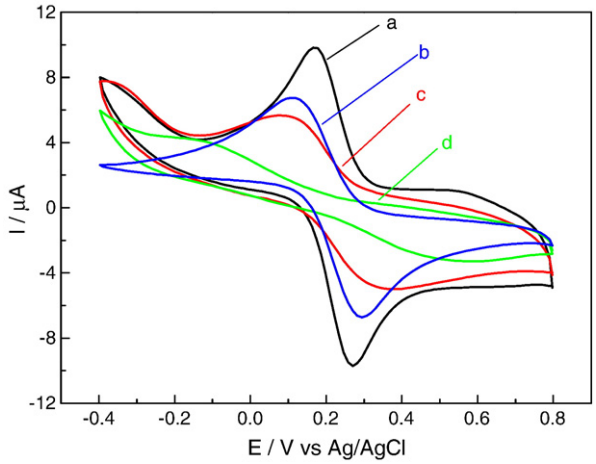

Fig. 3. Cyclic voltammogram obtained in 1 mM $K_3Fe(CN)_6$ + 0.1 M KCl solution for probe DNA immobilized (c and d) and not (a and b) on the planar gold (b and d) and Au NP modified planar electrode (a and c). The Au NP modified planar electrode was obtained with the electroless deposition in 1 mM $HAuCl_4$ for 6 min. Scan rates were all 100 mV/s.

immobilization of probe DNA on electrode surface induced a large decrease of peak current and an increase of peak to peak potential separation, indicating that probe DNA has been successfully immobilized on the electrode surface. The peak current decrease could be well assigned to the repellence of $[Fe(CN)_6^{3-/4-}]$ by the negatively charged phosphate backbone of probe DNA. Furthermore, it was interestingly found that the extent of peak current decrease after probe DNA immobilization occurring on the planar gold electrode was more pronounced than that on the Au NP modified electrode. This could be explained by the fact that probe DNA assembled on the Au NP modified electrode took a different orientation due to the small curvature radius effect of gold nanoparticle. Whereas, on the planar gold electrode, the self-assembly monolayer of probe DNA was considered to pack more densely and could block the diffusion of ferricyanide toward the electrode surface to a large extent.

Since Tarlov et al. firstly reported an effective way to quantitatively measure DNA surface density by using RuHex as a redox probe [39,40], this method has been widely used to characterize DNA immobilization and hybridization on the electrode surface. Cyclic voltammetry was firstly employed to characterize the electrochemistry of RuHex at probe DNA or dsDNA modified planar or Au NP electrode. At 50 μM RuHex, two pairs of well-defined peaks were observed for the probe DNA and MCH mixed monolayer modified planar gold electrode (Fig. 4, bottom). One peak occurring at the formal potential of about −0.12 V was ascribed to the diffusion of RuHex toward the electrode surface, while another peak at about −0.28 V arose due to the redox reaction of RuHex electrostatically bound to the phosphate backbone of DNA, which therefore could reflect the amount of DNA strands localized at the electrode surface. The peak currents for the pair of peaks at ~−0.28 V are linearly proportional to scan rates (data not shown), suggesting the characteristic of a surface-confined redox process. Also, the CV in blank Tris–HCl buffer solution after being immersed in 50 μM RuHex showed only one pair of peaks at ~−0.28 V (data not shown). While, only a pair of peaks at ~−0.12 V could be observed for MCH-only modified gold electrode.

The peak current at ~−0.28 V was found to be increased for the dsDNA assembled planar gold electrode than that of probe DNA only modified electrode. DNA hybridization introduces more negative charges of electrode surface which could trap more amount of RuHex for the electrochemical responses. Therefore, this peak current difference before and after DNA hybridization could reflect the DNA hybridization efficiency. The peak current at ~−0.28 V was found to be largely increased onto Au NP modified planar and PEM electrode (Fig. 4, middle and top). This could be attributed to the Au NP modification largely increasing the electrode surface area and then the immobilized and hybridized DNA amount.

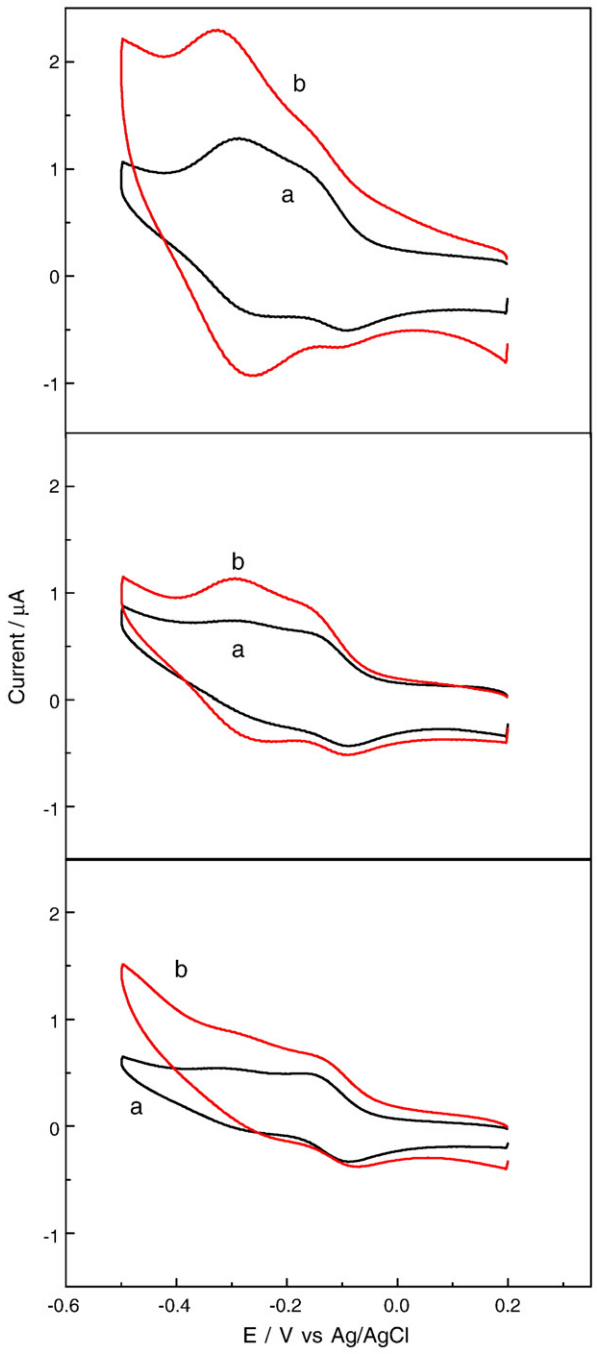

Fig. 4. Cyclic voltammogram of 50 μM RuHex in 0.2 M Tris–HCl solution (pH 7.4) for probe DNA immobilized (curve a) and DNA hybridized (curve b) onto the planar gold (bottom) and Au NP modified planar (middle) and PEM electrodes (top). Scan rates were all 100 mV/s. 1×10^{-5} M target DNA in PBS buffer (pH 6.83, 50 mM NaCl) was used for DNA hybridization. The Au NP modified planar and PEM electrodes were obtained by electroless deposition in 1 mM $HAuCl_4$ for 6 min.

To further demonstrate the DNA immobilization and hybridization onto different modified electrode surfaces, the differential pulse voltammetry (DPV) experiments were carried out with the RuHex as a redox label. DPV was commonly used because it could alleviate the background current effect to a large extent. The DPV results obtained in 3.5 μM RuHex were shown in Fig. 5. Due to the low concentration of RuHex advised, there was only a peak at about −0.28 V, which was the same as observed with CV experiment for the surface-confined redox process. The probe DNA modification on the planar gold electrode induced the peak current of about 0.34 μA when the

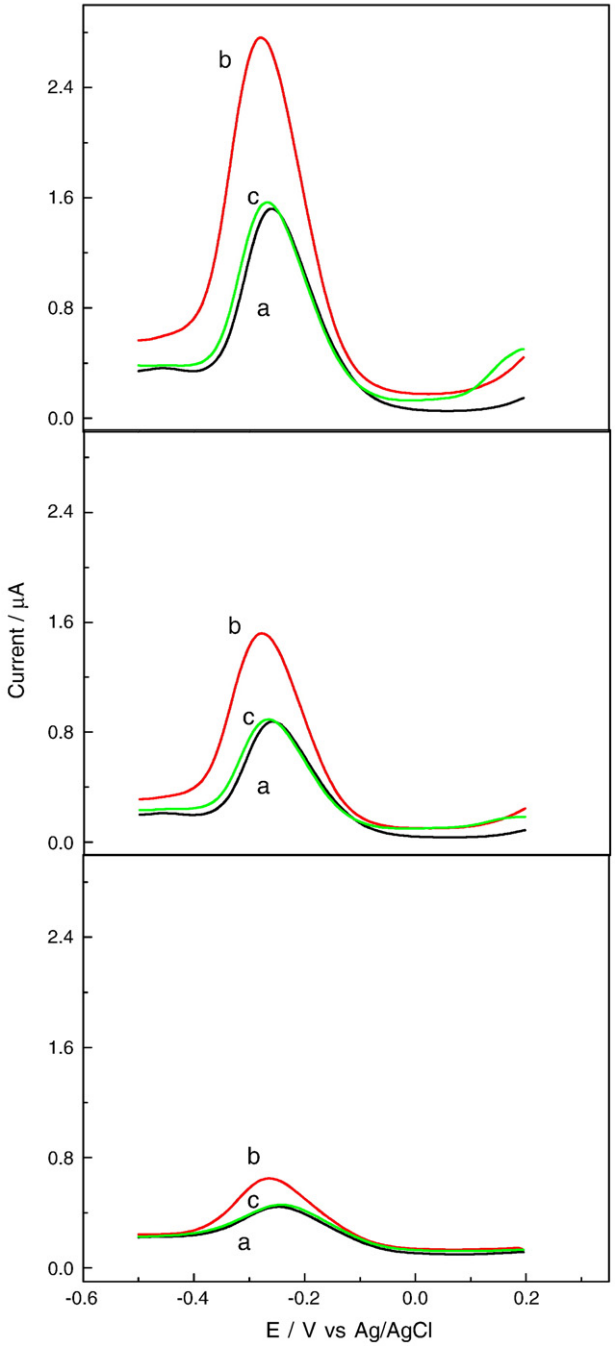

Fig. 5. Differential pulse voltammogram of 3.5 μM RuHex in 0.2 M Tris–HCl solution (pH 7.4) for probe DNA immobilized (curve a) and hybridized with complementary target DNA (curve b) and non-complementary target DNA (curve c) onto the planar gold (bottom) and Au NP modified planar (middle) and PEM electrodes (top). Scan rates were all 100 mV/s. The complementary and non-complementary target DNAs used for DNA hybridization were both 1×10^{-5} M in PBS buffer (pH 6.83, 50 mM NaCl). The Au NP modified planar and PEM electrodes were obtained by electroless deposition in 1 mM $HAuCl_4$ for 6 min.

background current was subtracted. The peak current increase of about 0.18 μA was observed when the hybridization of probe DNA modified electrode with target DNA. The hybridization efficiency on the planar gold electrode could be speculated to be about 53%. The peak current for the probe DNA immobilized onto Au NP modified planar electrode was about 0.85 μA. The peak current increase after DNA hybridization was about 0.58 μA, indicating a hybridization efficiency of about 68%. The peak current produced with the immobilization of probe DNA on the Au NP modified PEM electrode was about 1.47 μA and the peak current increase after DNA hybridization was about 1.11 μA. Thus, the hybridization efficiency was upgraded to be about 75% on the Au NP modified PEM electrode. It could be easily obtained that the immobilization amount of probe DNA on the Au NP modified PEM electrode or Au NP modified planar electrode was about 4.3 or 2.5 times of that on the planar gold electrode, respectively. Comparing the surface area increase for the Au NP modified electrodes and planar electrode, the increase of the probe DNA immobilization amount on Au NP modified electrodes was more prominent. The hybridization efficiency on the Au NP modified electrodes was also found to be evidently increased compared with that of planar gold electrode. This could be attributed that the small curvature radius of Au NPs offered a beneficial three dimensional environment for DNA immobilization and hybridization. Mirkin et al. have recently pointed out the influence of curvature radius of gold nanoparticles on DNA immobilization and hybridization [46]. This was also in good agreement with the observation for the electron transfer of ferricyanide through probe DNA immobilized on the planar and Au NP modified electrode. The control experiments for DNA hybridization were performed using a non-complementary target DNA sequence. No or negligible DPV peak current response was observed on the planar and Au NP modified electrode, indicating a good selectivity of current DNA biosensor. The relationship of DNA biosensor performance with different DNA hybridization times was also investigated on the Au NP modified PEM electrode (see Fig. S3 in the Appendix A). The DPV peak current of RuHex was found to increase with the hybridization time and a maximum current response could be obtained at about 1 h. Thus, the optimized DNA hybridization time was chosen as 1 h.

3.3. Detection limit for target DNA on Au NP modified electrode

The sensitivity of the electrochemical hybridization assay was further investigated by varying the target DNA concentration by DPV experiments with the use of RuHex as an indicator. The relation of DPV peak current increase (ΔI) of 3.5 μM RuHex with decrease in the concentration of target DNA on Au NP modified PEM electrode is displayed in Fig. 6. The sensitivity of Au NP modified PEM electrode for complementary target DNA could reach 10^{-11} mol/L. Three independent electrodes were used simultaneously for the acquisition of each point in the calibration curve. But on the planar gold electrode, the detection limit for target DNA could only be obtained as 10^{-8} mol/L.

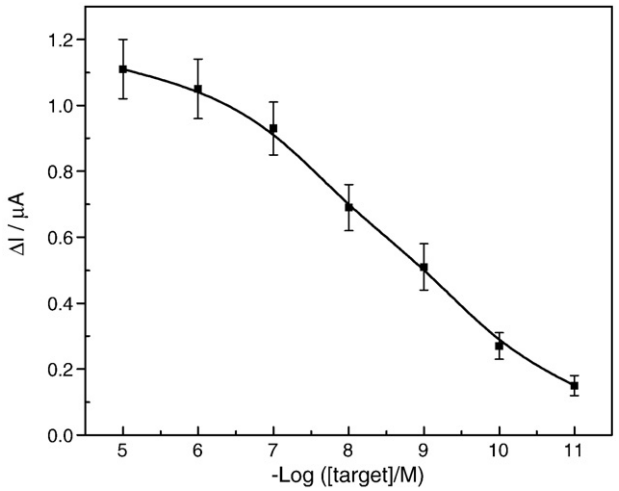

Fig. 6. Relation of the DPV peak current increase (ΔI) of 3.5 μM RuHex onto Au NP modified PEM electrode before and after DNA hybridization with target DNA concentration from 1×10^{-5} M to 1×10^{-11} M. Each point was obtained with three repetitive experiments. The Au NP modified PEM electrodes were obtained with the electroless deposition in 1 mM $HAuCl_4$ for 6 min.

Thus, the sensitivity for the detection of target DNA was increased about 3 orders of magnitude with the advisement of Au NPs by electroless deposition on the planar gold electrode. The regeneration for the DNA hybridized electrode was also investigated. It was found that the fabricated DNA biosensor could be conveniently regenerated by incubation of modified electrodes in hot water (80 °C) for 10 min, which completely removed hybridized DNA via thermal denaturation. The DNA biosensor almost retained its original performance after three regeneration cycles, with negligible loss of probes and without sacrificing hybridization efficiency (data not shown).

4. Conclusion

The current article provides a simple strategy for Au NP modification onto different conductive substrates and the Au NPs deposited could be easily controlled to some extent by choosing different solution concentrations, deposition times, etc. Furthermore, the sensitivity of fabricated electrochemical DNA biosensor toward target DNA could reach 1×10^{-11}M. Such a low detection limit makes it to be a good candidate for the application in clinical analysis, etc. Also, the current electrode modification method shows a good prospect in the application of immunosensor, enzyme biosensor and etc.

Acknowledgement

We thank the Natural Science Foundation of Shandong (grant number Q2008B05) for its financial supports.

Appendix A. Supplementary data

Supplementary data associated with this article can be found, in the online version, at doi:10.1016/j.bioelechem.2009.10.005.

References

[1] K.M. Millan, S.R. Mikkelsen, Sequence selective biosensor for DNA based on electroactive hybridization indicators, Anal. Chem. 65 (1993) 2317–2323.
[2] X. Lou, M.S. Lewis, C.B. Gorman, L. He, Detection of DNA point mutation by atom transfer radical polymerization, Anal. Chem. 77 (2005) 4698–4705.
[3] C. Fang, Y. Fan, J. Kong, Z. Gao, N. Balasubramanian, Electrical detection of oligonucleotide using an aggregate of gold nanoparticles as a conductive tag, Anal. Chem. 80 (2008) 9387–9394.
[4] J. Miao, Z. Cao, Y. Zhou, C. Lau, J. Lu, Instantaneous derivatization technology for simultaneous and homogeneous determination of multiple DNA targets, Anal. Chem. 80 (2008) 1606–1613.
[5] L. Zhang, C.Z. Huang, Y.F. Li, S.J. Xiao, J.P. Xie, Label-free detection of sequence-specific DNA with multiwalled carbon nanotubes and their light scattering signals, J. Phys. Chem. B 112 (2008) 7120–7122.
[6] W. Zheng, L. He, Label-free, real-time multiplexed DNA detection using fluorescent conjugated polymers, J. Am. Chem. Soc. 131 (2009) 3432–3433.
[7] Z. Gao, N.C. Tansil, An ultrasensitive photoelectrochemical nucleic acid biosensor, Nucleic Acids Res. 33 (2005) e123.
[8] I. Mannelli, M. Minunni, S. Tombelli, M. Mascini, Quartz crystal microbalance (QCM) affinity biosensor for genetically modified organisms (GMOs) detection, Biosens. Bioelectron. 18 (2003) 129–140.
[9] H. Shiigi, S. Tokonami, H. Yakabe, T. Nagaoka, Label-free electronic detection of DNA-hybridization on nanogapped gold particle film, J. Am. Chem. Soc. 127 (2005) 3280–3281.
[10] G. March, V. Noe¨l, B. Piro, S. Reisberg, M. Pham, Nanometric layers for direct, signal-on, selective, and sensitive electrochemical detection of oligonucleotides hybridization, J. Am. Chem. Soc. 130 (2008) 15752–15753.
[11] J. Zhang, S. Song, L. Zhang, L. Wang, H. Wu, D. Pan, C. Fan, Sequence-specific detection of femtomolar DNA via a chronocoulometric DNA sensor (CDS): effects of nanoparticle-mediated amplification and nanoscale control of DNA assembly at electrodes, J. Am. Chem. Soc. 128 (2006) 8575–8580.
[12] E. Kim, K. Kim, H. Yang, Y.T. Kim, J. Kwak, Enzyme-amplified electrochemical detection of DNA using electrocatalysis of ferrocenyl-tethered dendrimer, Anal. Chem. 75 (2003) 5665–5672.
[13] M.R. Gore, V.A. Szalai, P.A. Ropp, I.V. Yang, J.S. Silverman, H.H. Thorp, Detection of attomole quantities of DNA targets on gold microelectrodes by electrocatalytic nucleobase oxidation, Anal. Chem. 75 (2003) 6586–6592.
[14] J.A. Hansen, R. Mukhopadhyay, J.Ø. Hansen, K.V. Gothelf, Femtomolar electrochemical detection of DNA targets using metal sulfide nanoparticles, J. Am. Chem. Soc. 128 (2006) 3860–3861.
[15] K. Lee, K. Maisel, J. Rouillard, E. Gulari, J. Kim, Sensitive and selective label-free DNA detection by conjugated polymer-based microarrays and intercalating dye, Chem. Mater. 20 (2008) 2848–2850.
[16] T.M. Lee, L. Li, I. Hsing, Enhanced electrochemical detection of DNA hybridization based on electrode-surface modification, Langmuir 19 (2003) 4338–4343.
[17] S. Hwang, E. Kim, J. Kwak, Electrochemical detection of DNA hybridization using biometallization, Anal. Chem. 77 (2005) 579–584.
[18] G. Farace, G. Lillie, T. Hianik, P. Payne, P. Vadgama, Reagentless biosensing using electrochemical impedance spectroscopy, Bioelectrochemistry 55 (2002) 1–3.
[19] S. Reisberga, B. Piroa, V. Noela, M.C. Pham, Selectivity and sensitivity of a reagentless electrochemical DNA sensor studied by square wave voltammetry and fluorescence, Bioelectrochemistry 69 (2006) 172–179.
[20] V. Ostatná, N. Dolinnaya, S. Andreev, T. Oretskaya, J. Wang, T. Hianik, The detection of DNA deamination by electrocatalysis at DNA-modified electrodes, Bioelectrochemistry 67 (2005) 205–210.
[21] T.G. Drummond, M.G. Hill, J.K. Barton, Electrochemical DNA sensors, Nat. Biotechnol. 21 (2003) 1192–1199.
[22] J. Zhang, R. Lao, S. Song, Z. Yan, C. Fan, Design of an oligonucleotide-incorporated nonfouling surface and its application in electrochemical DNA sensors for highly sensitive and sequence-specific detection of target DNA, Anal. Chem. 80 (2008) 9029–9903.
[23] E.L.S. Wong, E. Chow, J.J. Gooding, DNA recognition interfaces: the influence of interfacial design on the efficiency and kinetics of hybridization, Langmuir 21 (2005) 6957–6965.
[24] R. Lao, S. Song, H. Wu, L. Wang, Z. Zhang, L. He, C. Fan, Electrochemical interrogation of DNA monolayers on gold surfaces, Anal. Chem. 77 (2005) 6475–6480.
[25] R. Levicky, T.M. Herne, M.J. Tarlov, S.K. Satija, Using self-assembly to control the structure of DNA monolayers on gold: a neutron reflectivity study, J. Am. Chem. Soc. 120 (1998) 9787–9792.
[26] E.L.S. Wong, J.J. Gooding, Charge transfer through DNA: a selective electrochemical DNA biosensor, Anal. Chem. 78 (2006) 2138–2144.
[27] J. Li, H.T. Ng, A. Cassell, W. Fan, H. Chen, Q. Ye, J. Koehne, J. Han, M. Meyyappan, Carbon nanotube nanoelectrode array for ultrasensitive DNA detection, Nano Lett. 3 (2003) 597–602.
[28] A. Erdem, P. Papakonstantinou, H. Murphy, Direct DNA hybridization at disposable graphite electrodes modified with carbon nanotubes, Anal. Chem. 78 (2006) 6656–6659.
[29] Z. Li, Y. Chen, X. Li, T.I. Kamins, K. Nauka, R.S. Williams, Sequence-specific label-free DNA sensors based on silicon nanowires, Nano Lett. 4 (2004) 245–247.
[30] I. Willner, B. Willner, E. Katz, Biomolecule–nanoparticle hybrid systems for bioelectronic applications, Bioelectrochemistry 70 (2007) 2–11.
[31] C. Li, Y. Liu, J.H.T. Luong, Impedance sensing of DNA binding drugs using gold substrates modified with gold nanoparticles, Anal. Chem. 77 (2005) 478–485.
[32] D. Li, Y. Yan, A. Wieckowska, I. Willner, Amplified electrochemical detection of DNA through the aggregation of Au nanoparticles on electrodes and the incorporation of methylene blue into the DNA-crosslinked structure, Chem. Commun. 34 (2007) 3544–3546.
[33] H. Cai, C. Xu, P. He, Y. Fang, Colloid Au-enhanced DNA immobilization for the electrochemical detection of sequence-specific DNA, J. Electroanal. Chem. 510 (2001) 78–85.
[34] S. Liu, Y. Li, J. Li, L. Jiang, Enhancement of DNA immobilization and hybridization on gold electrode modified by nanogold aggregates, Biosens. Bioelectron. 21 (2005) 789–795.
[35] T. Liu, J.A. Tang, H.Q. Zhao, Y.P. Deng, L. Jiang, Particle size effect of the DNA sensor amplified with gold nanoparticles, Langmuir 18 (2002) 5624–5626.
[36] L.A. Porter, H.C. Choi, A.E. Ribbe, J.M. Buriak, Controlled electroless deposition of noble metal nanoparticle films on germanium surfaces, Nano lett. 2 (2002) 1067–1071.
[37] S. Liu, J. Li, L. Jiang, Surface modification of platinum quartz crystal microbalance by controlled electroless deposition of gold nanoparticles and its enhancing effect on the HS-DNA immobilization, Colloids Surf. A: Physicochem. Eng. Asp. 257–258 (2005) 57–62.
[38] A. Hilmi, J.H.T. Luong, Electrochemical detectors prepared by electroless deposition for microfabricated electrophoresis chips, Anal. Chem. 72 (2000) 4677–4682.
[39] A.B. Steel, T.M. Herne, M.J. Tarlov, Electrochemical quantification of DNA immobilized on gold, Anal. Chem. 70 (1998) 4670–4677.
[40] L. Su, C.G. Sankar, D. Sen, H. Yu, Kinetics of ion-exchange binding of redox metal cations to thiolate-DNA monolayers on gold, Anal. Chem. 76 (2004) 5953–5959.
[41] X. Zhang, F. Shi, X. Yu, H. Liu, Y. Fu, Z.Q. Wang, L. Jiang, X.Y. Li, Polyelectrolyte multilayer as matrix for electrochemical deposition of gold clusters: toward super-hydrophobic surface, J. Am. Chem. Soc. 126 (2004) 3064–3065.
[42] N. Zhao, F. Shi, Z. Wang, X. Zhang, Combining layer-by-layer assembly with electrodeposition of silver aggregates for fabricating superhydrophobic surfaces, Langmuir 21 (2005) 4713–4716.
[43] L. Qian, X. Yang, Polyamidoamine dendrimers-assisted electrodeposition of gold–platinum bimetallic nanoflowers, J. Phys. Chem. B 110 (2006) 16672–16678.
[44] L. Qian, Y. Liu, Y. Song, Z. Li, X. Yang, Electrodeposition of Pt nanoclusters on the surface modified by monolayer poly(amidoamine) dendrimer film, Electrochem. Commun. 7 (2005) 1209–1212.
[45] S. Trasatti, O.A. Petrii, Real surface area measurements in electrochemistry, J. Electroanal. Chem. 327 (1992) 353–376.
[46] H.D. Hill, J.E. Millstone, M.J. Banholzer, C.A. Mirkin, The role radius of curvature plays in thiolated oligonucleotide loading on gold nanoparticles, ACS Nano 3 (2009) 418–424.